

# Morphology, Structure, and Conductivity of Polypyrrole Prepared in the Presence of Mixed Surfactants in Aqueous Solutions

Shuangxi Xing, Guoku Zhao

Faculty of Chemistry, Northeast Normal University, Changchun 130024, People's Republic of China

Received 20 October 2006; accepted 7 December 2006

DOI 10.1002/app.25912

Published online in Wiley InterScience (www.interscience.wiley.com).

**ABSTRACT:** Polypyrrole (PPy) was prepared from different mixed-surfactant solutions with ammonium persulfate as an oxidant. Three types of combinations were selected, including cationic/anionic, cationic/nonionic, and anionic/nonionic mixed-surfactant solutions. The surfactants used in the experiments included cetyltrimethylammonium bromide (cationic surfactant), sodium dodecyl sulfate (anionic surfactant), sodium dodecyl sulfonic acid salt (anionic surfactant), poly(vinyl pyrrolidone) (nonionic surfactant), and poly(ethylene glycol) (nonionic surfactant). The morphology, structure, and conductivity of the resulting PPy were investigated in detail with scanning electron microscopy, Fourier transform infrared spectra, and the typical four-probe method, respectively. The results showed that the interaction between the different surfactants and the interaction between the surfactants and the

polymer influenced the morphology, structure, and conductivity of the resulting polymer to different degrees. The cationic surfactant favored the formation of nanofibers, the addition of anionic surfactants produced agglomeration but enhanced the doping level and conductivity, and the presence of a nonionic surfactant weakened the interaction between the other surfactant and the polymer in the system. In comparison with the results for monosurfactant solutions, the polymerization of pyrrole in mixed-surfactant solutions could modulate the morphologies of PPy, which ranged from nanofibers of different lengths to nanoparticles showing various states of aggregation. © 2007 Wiley Periodicals, Inc. *J Appl Polym Sci* 104: 1987–1996, 2007

**Key words:** conducting polymers; morphology; polypyrroles; structure; surfactants

## INTRODUCTION

In recent years, polypyrrole (PPy), as one of the most promising conducting polymers, has received comprehensive interest because of its excellent characteristics, including easy preparation, environmental stability, and high conductivity. These merits have led PPy to have wide potential applications in various fields, such as sensors, actuators, and electric devices.<sup>1–4</sup> Therefore, obtaining PPy with excellent chemical and physical characteristics becomes more and more attractive. For this purpose, the polymerization of pyrrole in different surfactant systems has been developed quickly because surfactants can induce pyrrole to grow in a certain manner and result in PPy with an ordered morphology, which will show properties superior to those from a conventional aqueous solution.<sup>5,6</sup> On the other hand, the doping of the surfactant into the polymer backbone can improve the thermo-

stability of the resulting products.<sup>7,8</sup> Among the conventional surfactants, cetyltrimethylammonium bromide (CTAB) has proved to be the most effective for guiding the formation of PPy nanofibers.<sup>9,10</sup> Zhang et al.<sup>11</sup> investigated the controllable synthesis of PPy nanostructures with different kinds of surfactants, including CTAB, dodecyltrimethylammonium (DTAB), octyltrimethylammonium, poly(ethylene glycol) monononylphenyl ether, and sodium dodecyl sulfate (SDS). They showed that a wirelike ribbon was obtained when CTAB, DTAB, and ammonium persulfate (APS) were used, but only a spherelike structure was obtained under other conditions, except that PPy without a geometrical nanofeature was generated when SDS was used. Grady et al.<sup>12</sup> reported the formation of nanostructured PPy with controlled morphologies on atomically flat surfaces with adsorbed surfactant molecules as templates. Omastová et al.<sup>13</sup> investigated the synthesis and structure of PPy prepared in the presence of surfactants, including anionic, cationic, and nonionic types of surfactants, in detail. They found that the anionic surfactants would incorporate into the PPy chain as dopants, leading to the improvement of the conductivity and stability of the products. Although a lot of publications have reported investigations of the preparation of PPy in different surfac-

Correspondence to: S. Xing (xingsx737@nenu.edu.cn).

Contract grant sponsor: Science Foundation for Young Teachers of Northeast Normal University; contract grant number: 20060312.

tants, as listed previously, few reports have been found on the preparation of PPy prepared in the presence of mixed surfactants, such as anionic/cationic and anionic/nonionic surfactant systems. Indeed, inorganic nanoparticles with special morphologies and properties have already been prepared from mixed-surfactant solutions. For example, star-shaped PbS nanocrystals have been synthesized in aqueous solutions of mixed CTAB/SDS surfactants, and the mixed CTAB/SDS surfactants may have played the role of binary capping agents in the nucleation and growth of PbS crystals, leading to the gradual growth of star-shaped PbS nanocrystals during the early reaction stages.<sup>14</sup> Therefore, we carried out the polymerization of pyrrole in different types of mixed-surfactant solutions to investigate the interaction between the different surfactants and the interaction between the surfactants and the polymer. The influences of different preparation conditions on the properties of the resulting PPy were also examined.

## EXPERIMENTAL

### Materials

Pyrrole was distilled *in vacuo* before use, and other reagents, including APS, CTAB, SDS, sodium dodecyl

sulfonic acid salt (SDSA), poly(vinyl pyrrolidone) (PVP; weight-average molecular weight  $\approx$  30,000), and poly(ethylene glycol) (PEG; weight-average molecular weight  $\approx$  19,000), were used as received.

### Preparation of PPy

The preparation of PPy in CTAB/SDS mixed-surfactant solutions with a molar ratio of 6 : 1 is described as an example: 0.432 g of CTAB and 0.058 g of SDS were codissolved in 100 mL of deionized water. After the solution became transparent, 0.35 mL of pyrrole was added. Then, 1.14 g of ground APS powder was directly dissolved in this solution and initiated the polymerization of pyrrole. The mixture was stirred at room temperature for 6 h, and the resulting precipitate was collected by filtration or centrifugation. After the product was washed with deionized water and ethanol, the product was dried *in vacuo* at 60°C for 24 h. The other preparation conditions are listed in detail in Table I.

### Characterization

The morphologies of the samples were observed with scanning electron microscopy (SEM; SSX-550, Shimadzu, Japan) with a gold coating.

**TABLE I**  
Preparation Conditions for PPy in Different Monosurfactant and Mixed-Surfactant Solutions and Corresponding FTIR Data and Conductivity Values

No.	Surfactant	Usage (g)	Molar ratio	Mass ratio	Peak position ( $\text{cm}^{-1}$ )		$A_2/A_1$	Conductivity (S/cm)
					1	2		
1	CTAB	0.432	—	—	1568	1483	0.117	1.11
2	SDS	0.348	—	—	1544	1453	0.202	—
3	SDSA	0.324	—	—	1543	1440	0.250	—
4	PEG	0.432	—	—	1554	1471	0.159	2.07
5	PVP	0.432	—	—	1550	1464	0.178	1.56
6	CTAB/SDS	0.432/0.058	6 : 1	—	1562	1478	0.149	0.89
7	CTAB/SDS	0.432/0.116	3 : 1	—	1564	1479	0.099	0.50
8	CTAB/SDS	0.432/0.348	1 : 1	—	1558	1465	0.350	1.49
9	CTAB/SDS	0.144/0.348	1 : 3	—	1543	1463	0.329	8.51
10	CTAB/SDS	0.072/0.348	1 : 6	—	1543	1461	0.268	—
11	CTAB/SDSA	0.432/0.054	6 : 1	—	1554	1474	0.100	0.83
12	CTAB/SDSA	0.432/0.108	3 : 1	—	1556	1469	0.137	1.00
13	CTAB/SDSA	0.432/0.324	1 : 1	—	1558	1467	0.184	3.08
14	CTAB/SDSA	0.144/0.324	1 : 3	—	1548	1463	0.307	5.24
15	CTAB/SDSA	0.072/0.324	1 : 6	—	1547	1458	0.273	—
16	CTAB/PEG	0.432/0.216	—	2 : 1	1567	1482	0.091	1.02
17	CTAB/PEG	0.432/0.432	—	1 : 1	1566	1481	0.103	0.64
18	CTAB/PEG	0.432/0.864	—	1 : 2	1562	1478	0.106	0.74
19	CTAB/PVP	0.432/0.216	—	2 : 1	1558	1479	0.144	1.00
20	CTAB/PVP	0.432/0.432	—	1 : 1	1556	1478	0.180	1.17
21	CTAB/PVP	0.432/0.864	—	1 : 2	1560	1476	0.138	0.94
22	SDS/PEG	0.348/0.174	—	2 : 1	1542	1452	0.276	—
23	SDS/PEG	0.348/0.348	—	1 : 1	1550	1456	0.185	—
24	SDS/PEG	0.348/0.696	—	1 : 2	1544	1457	0.161	—
25	SDS/PVP	0.348/0.174	—	2 : 1	1542	1443	0.401	—
26	SDS/PVP	0.348/0.348	—	1 : 1	1548	1431	1.01	—

Fourier transform infrared (FTIR) spectra of the different samples were measured on an 8400s FTIR spectrometer (Shimadzu, Japan) in the absorption mode. The standard KBr technique was applied. The resolution of the measurements was  $4\text{ cm}^{-1}$ .

The conductivity of the powder pellets at room temperature was measured with the typical four-probe method (SDY-5, Guangzhou, China). For each value reported, at least three measurements were averaged.

## RESULTS AND DISCUSSION

### Morphology

The morphologies of PPy prepared from monocomponent surfactant systems can be found in Figure 1. Nanofibers are obtained only from a CTAB aqueous solution, and this is consistent with previous reports.<sup>9,10</sup> When SDS and SDSA are used, obvious agglomeration is found because of the strong interaction between the surfactants and the polymer. Globular particles are generated in PEG and PVP aqueous solutions. However, the particles in PVP are much smaller than those in the PEG solution, that is, about 80 vs 350 nm; this is quite similar to the results from the polymerization of pyrrole in the presence of poly(*N*-isopropylacrylamide-*co*-acrylamide).<sup>15</sup>

The SEM images of PPy obtained from CTAB/SDS mixed-surfactant solutions with molar ratios ranging from 6 : 1 to 1 : 6 are given in Figure 2. The addition of the anionic surfactant to the CTAB system shows an obvious effect on the morphology of PPy. The 1- $\mu\text{m}$  fibers in the CTAB monosolution are shortened to 500 nm when the molar ratio of CTAB to SDS is 6 : 1. When the molar ratio is down to 3 : 1, homogeneous nanoparticles with an average diameter of about 80 nm are obtained. The size of the particles becomes larger (ca. 180 nm) and agglomerates emerge when the ratio reaches 1 : 1. The agglomeration becomes serious with increasing usage of SDS because the electrostatic interaction between the PPy polycation and SDS is stronger than that between CTAB and SDS.

Meanwhile, the preparation of PPy in CTAB/SDSA mixed-surfactant solutions was also performed, and the SEM images of the resulting products are shown in Figure 3. Unlike the results from CTAB/SDS solutions, when the molar ratio of CTAB to SDSA is kept at 6 : 1, the products show little change in the morphology and size with respect to those obtained from CTAB solutions, and this may be assigned to the relatively weak counterions in SDSA versus those in SDS. Moreover, the nanofibers still exist when the ratio of CTAB to SDSA reaches 1 : 1, although serious agglomeration is observed when the ratio becomes lower than 1 : 1.

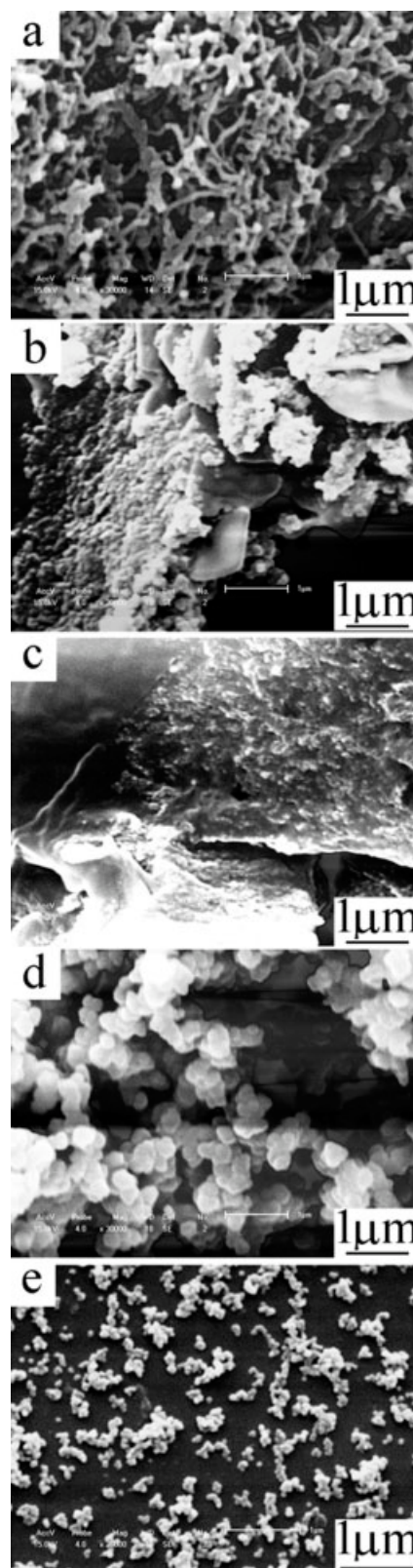


**Figure 1** SEM images of PPy prepared from different monosurfactant solutions: (a) CTAB, (b) SDS, (c) SDSA, (d) PEG, and (e) PVP.

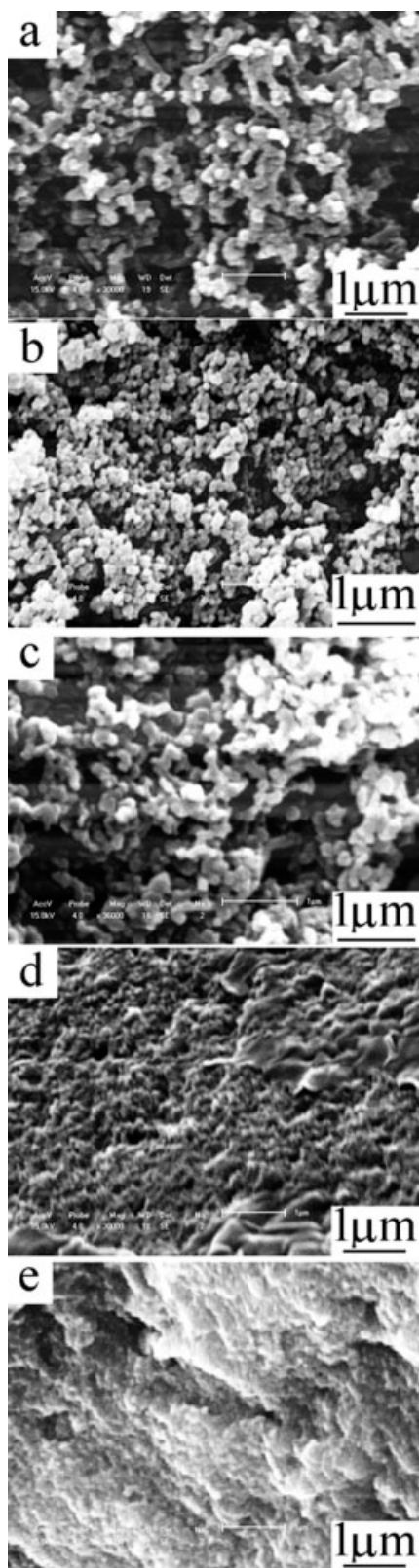


**Figure 2** SEM images of PPy prepared from CTAB/SDS mixed-surfactant solutions with different molar ratios: (a) 6 : 1, (b) 3 : 1, (c) 1 : 1, (d) 1 : 3, and (e) 1 : 6.

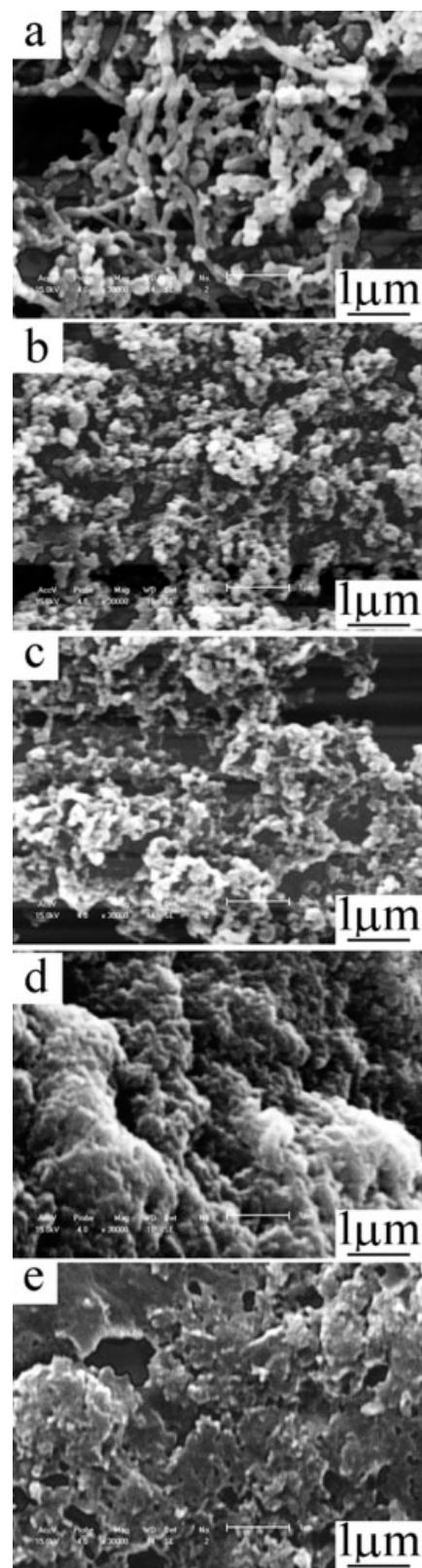


**Figure 3** SEM images of PPy prepared from CTAB/SDSA mixed-surfactant solutions with different molar ratios: (a) 6 : 1, (b) 3 : 1, (c) 1 : 1, (d) 1 : 3, and (e) 1 : 6.

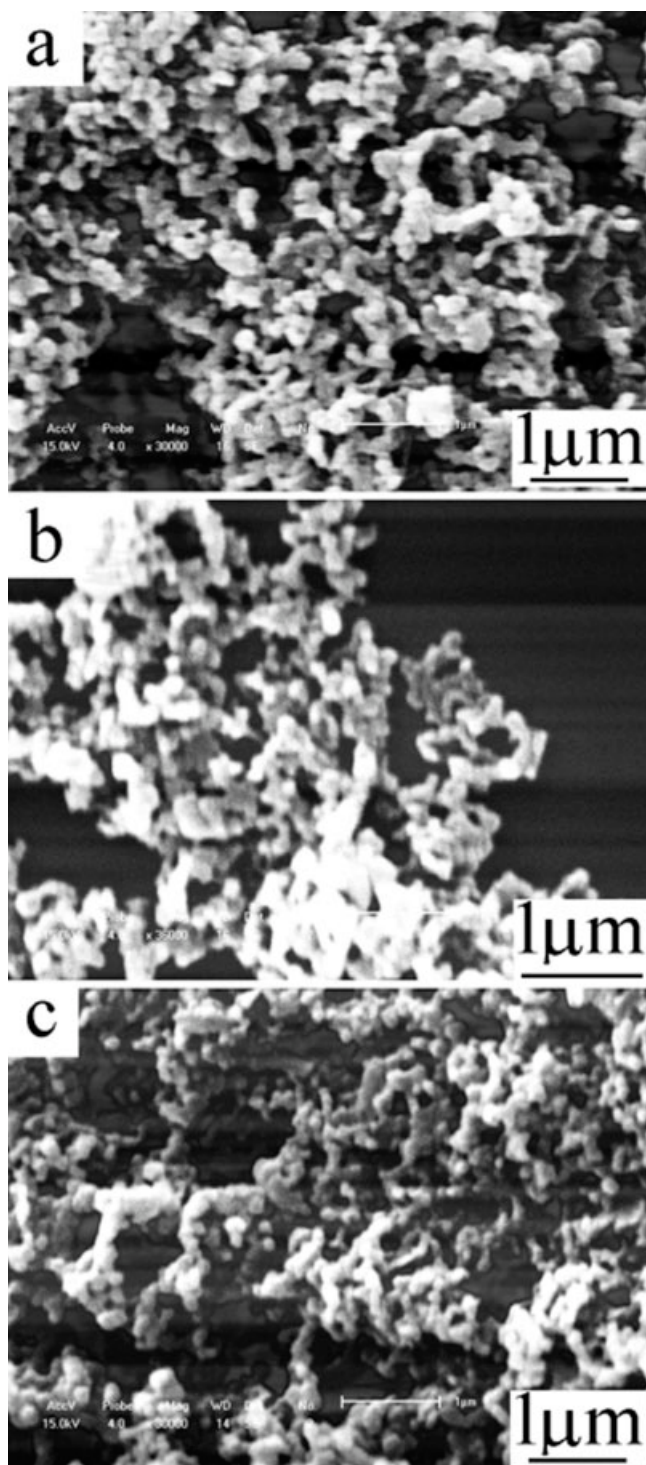


**Figure 4** SEM images of PPy prepared from CTAB/PEG mixed-surfactant solutions with different mass ratios: (a) 2 : 1, (b) 1 : 1, and (c) 1 : 2.

The SEM images of the resulting PPy from CTAB/PEG mixed-surfactant solutions with different mass ratios are presented in Figure 4. The length of the fibers is reduced by the addition of PEG, but little difference can be observed by changes in the usage of PEG. Simultaneously, some globular particles

adhere to the fibers with an average size of about 100 nm. Compared with the results shown in Figure 1(d), which presents the SEM image of PPy globular particles obtained from a monocomponent PEG solution, a smaller size is found, indicating that the inter-

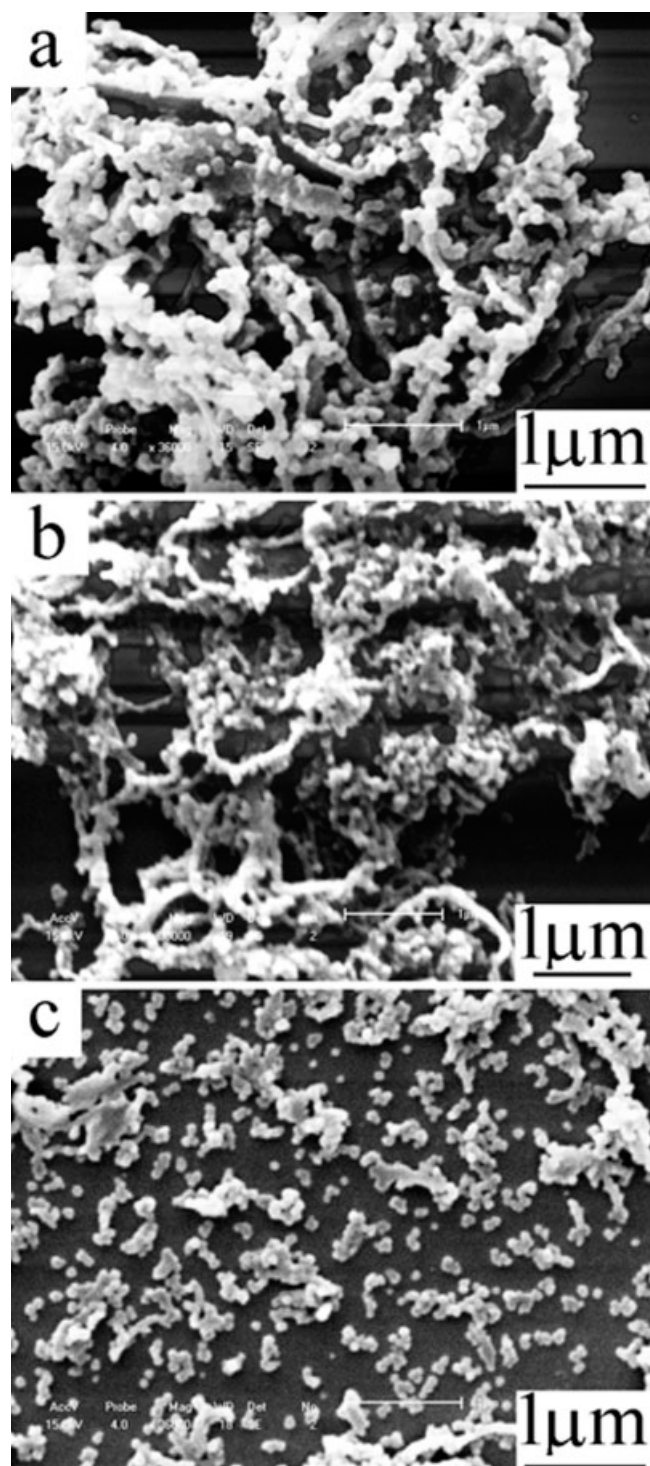


**Figure 5** SEM images of PPy prepared from CTAB/PVP mixed-surfactant solutions with different mass ratios: (a) 2 : 1, (b) 1 : 1, and (c) 1 : 2.

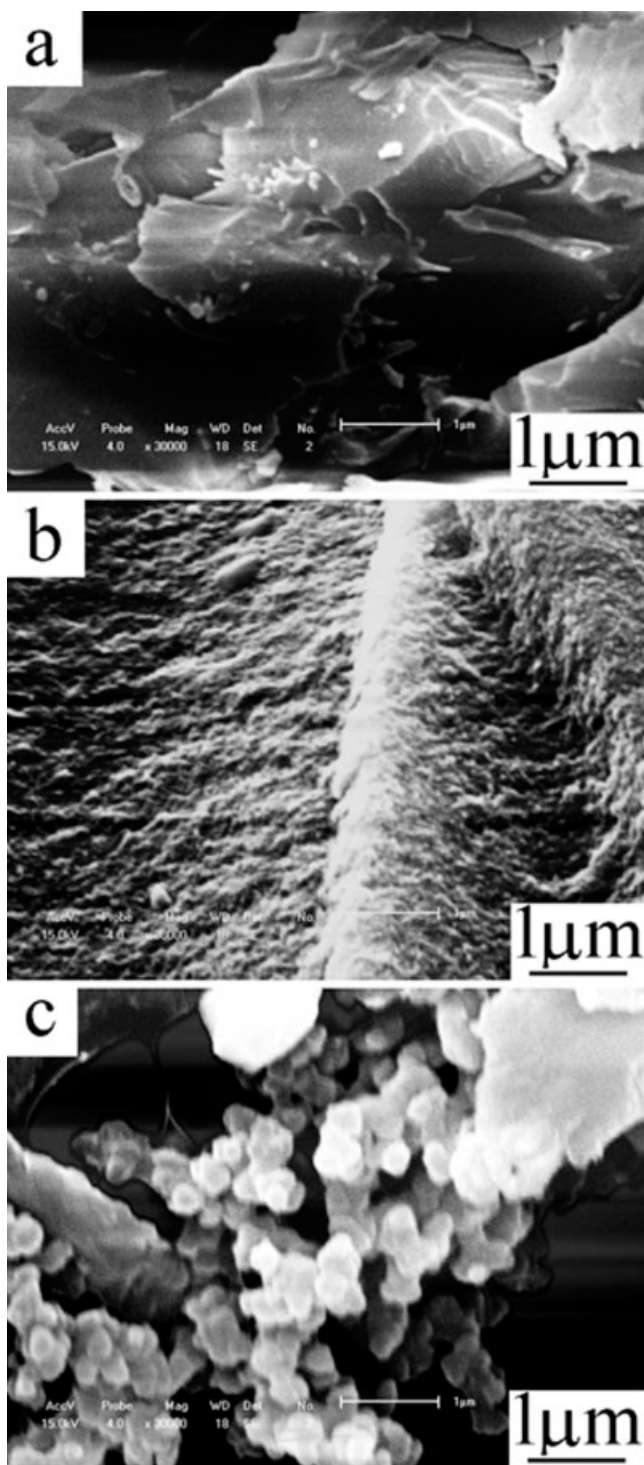


**Figure 6** SEM images of PPy prepared from SDS/PEG mixed-surfactant solutions with different mass ratios: (a) 2 : 1, (b) 1 : 1, and (c) 1 : 2.

action between CTAB and PEG influences the size of both the fibers and the particles.

On the other hand, when PPy is prepared from CTAB/PVP mixed solutions, nanofibers adsorbed with nanoparticles can also be observed, as shown in Figure 5(a,b). Unlike the results from the CTAB/

PEG systems, the size of the nanofibers and nanoparticles does not change much, and the nanofibers nearly disappear with increasing usage of PVP; a large number of nanoparticles with an average size of 80 nm predominate in the whole product [Fig. 5(c)]. This indicates that there may be less interaction between CTAB and PVP than between CTAB and PEG.

As can be seen in Figure 6, which presents SEM images of PPy obtained from SDS/PEG mixed-surfactant solutions with different mass ratios, the agglomeration can be alleviated with increased usage of PEG because the addition of PEG and its following dispersion in the reaction system may weaken the interaction between SDS and PPy. However, the particles show little difference in size from those obtained from a mono-PEG solution, as can be seen in Figure 6(c).

Although the different degrees of agglomeration of PPy prepared from SDS/PVP systems cannot be directly concluded from Figure 7(a,b), when the

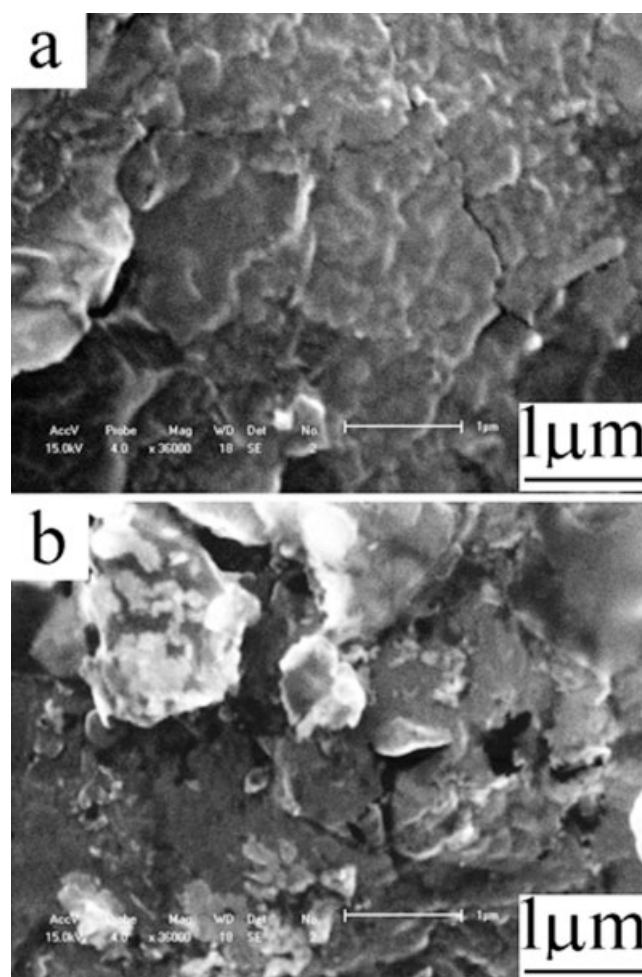


**Figure 7** SEM images of PPy prepared from SDS/PVP mixed-surfactant solutions with different mass ratios: (a) 2 : 1 and (b) 1 : 1.

mass ratio of SDS to PVP is less than 1 : 2, no precipitate but instead a PPy dispersion with high stability can be obtained, and we are presently investigating the formation and stability of the dispersions with different surfactant systems. Under this condition, even centrifugation with a rotation of 4000 rpm cannot produce precipitates, and this indicates the strong interaction between PVP, SDS, and PPy.

### FTIR spectra

The FTIR spectra of PPy obtained from different types of surfactants are shown in Figure 8, and the main peak positions are listed in Table I. The characteristic peaks of PPy can be clearly observed. For instance, the peaks at about 1570 and 1480  $\text{cm}^{-1}$  correspond to the C—C and C—N stretching vibrations in the pyrrole ring, respectively, which can also represent the antisymmetric and symmetric pyrrole ring stretching modes; the peak near 1194  $\text{cm}^{-1}$  corresponds to the breathing vibration of the pyrrole ring, and the peaks at about 1043 and 910  $\text{cm}^{-1}$  can be assigned to the C—H in-plane and out-of-plane deformation vibrations, respectively.<sup>16,17</sup> An additional peak at about 1700  $\text{cm}^{-1}$  can be observed for some samples [see Fig. 8(a,d)], indicating that PPy is slightly overoxidized during the growth process.<sup>18</sup> Besides, two weak peaks at 2924 and 2856  $\text{cm}^{-1}$  can be attributed to the stretching vibration mode of methylene in PPy prepared from SDS and SDSA solutions, indicating that these two anionic types of surfactants have been doped into the PPy structure [see Fig. 8(b,c)].<sup>11,16</sup>

It is well known that the doping of PPy affects the skeletal vibrations, and peak shifts can be observed

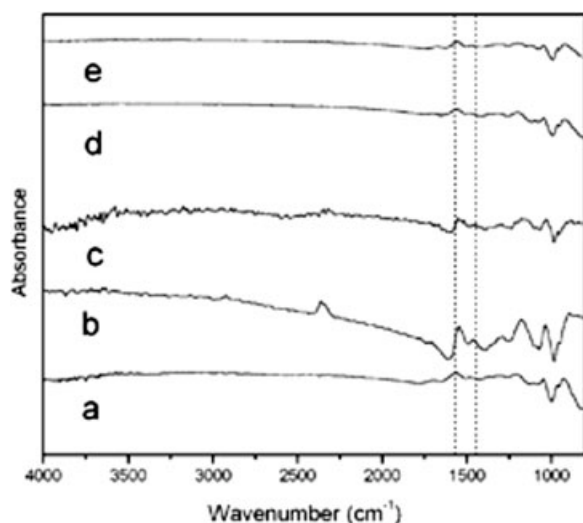


**Figure 8** FTIR spectra of PPy prepared from different monosurfactant solutions: (a) CTAB, (b) SDS, (c) SDSA, (d) PEG, and (e) PVP.

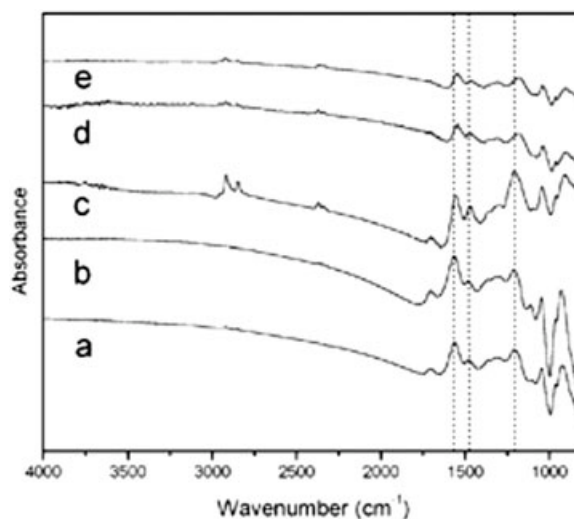


**Figure 9** FTIR spectra of PPy prepared from CTAB/SDS mixed-surfactant solutions with different molar ratios: (a) 6 : 1, (b) 3 : 1, (c) 1 : 1, (d) 1 : 3, and (e) 1 : 6.

directly from the FTIR spectrum. On the other hand, as the conjugation length increases, the intensity of the antisymmetric ring stretching mode at 1570  $\text{cm}^{-1}$  ( $A_1$  in Table I) will decrease, and the intensity of the symmetric mode at 1480  $\text{cm}^{-1}$  ( $A_2$  in Table I) will increase.<sup>19</sup> From Figure 8 and Table I, one can conclude that PPy obtained from a CTAB solution shows the lowest doping level and shortest conjugation length in comparison with PPy from other monosurfactant solutions because it gives the highest wave numbers of the main peaks and the lowest corresponding ratio of  $A_2$  to  $A_1$ . A further detailed discussion can be found in the following sections.

The FTIR spectra of PPy obtained from CTAB/SDS mixed-surfactant solutions with different molar ratios and the corresponding main peaks are shown in Figure 9 and Table I, respectively. The peaks around 1570 and 1480  $\text{cm}^{-1}$  show redshifting from 1562 and 1478  $\text{cm}^{-1}$  with a ratio of 6 : 1 to 1543 and 1461  $\text{cm}^{-1}$  with a ratio of 1 : 6, indicating the increasing doping level. Interestingly, PPy prepared from a system with a CTAB/SDS ratio of 3 : 1 gives the highest wave numbers and the lowest value of  $A_2/A_1$  among these five samples. We think that this abnormal result may be related to the stronger interaction between CTAB and SDS under this molar ratio, and the morphology of PPy from this system giving homogeneous particles also confirms the proposal [see Fig. 2(b)]. Apart from that, the ratio of  $A_2$  to  $A_1$  reaches its highest value when the molar ratio of 1 : 1 is used, and this indicates that the resulting PPy may have the longest conjugation chain. However, the value of  $A_2/A_1$  decreases with the molar ratio of CTAB to SDS. Therefore, we think that the anionic surfactant SDS improves the doping level of PPy because it can form an ionic bond with

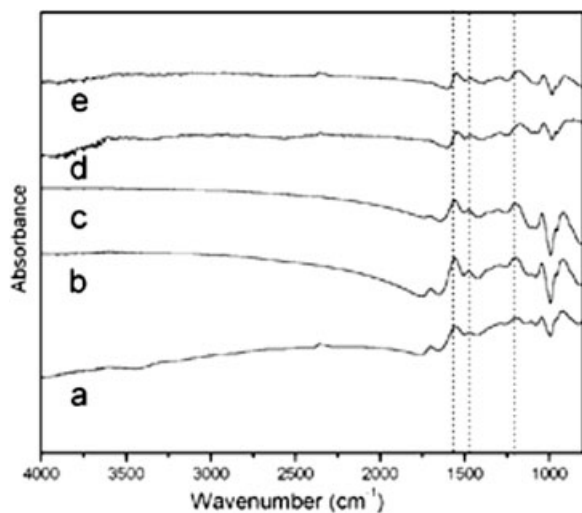


**Figure 10** FTIR spectra of PPy prepared from CTAB/SDSA mixed-surfactant solutions with different molar ratios: (a) 6 : 1, (b) 3 : 1, (c) 1 : 1, (d) 1 : 3, and (e) 1 : 6.

the PPy polycation. On the other hand, SDS is helpful for increasing the length of the conjugation chain, but it is not always true; on the contrary, too high an SDS concentration impedes the chain propagation.

Similar results can be found in CTAB/SDSA systems (see Fig. 10 and Table I), except for two conclusions: (1) no abnormal phenomenon has been observed in the redshift tendency of the main peaks, and (2) the highest value of  $A_2/A_1$  occurs at the CTAB/SDSA ratio of 1 : 3 and perhaps originates from the counterions of SDSA being weaker than those of SDS, as we have already discussed in the Morphology section.

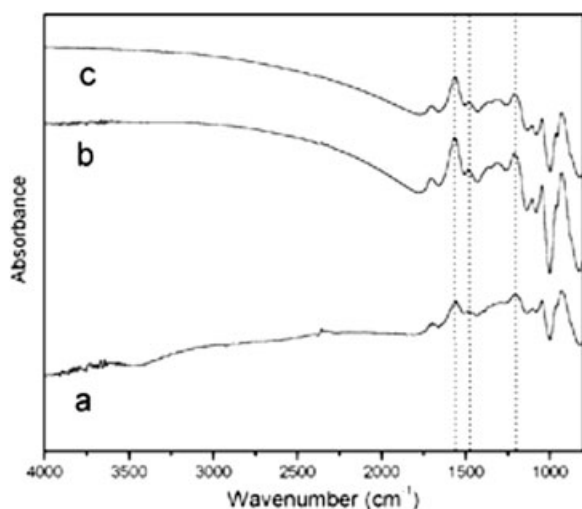


**Figure 11** FTIR spectra of PPy prepared from CTAB/PEG mixed-surfactant solutions with different mass ratios: (a) 2 : 1, (b) 1 : 1, and (c) 1 : 2.

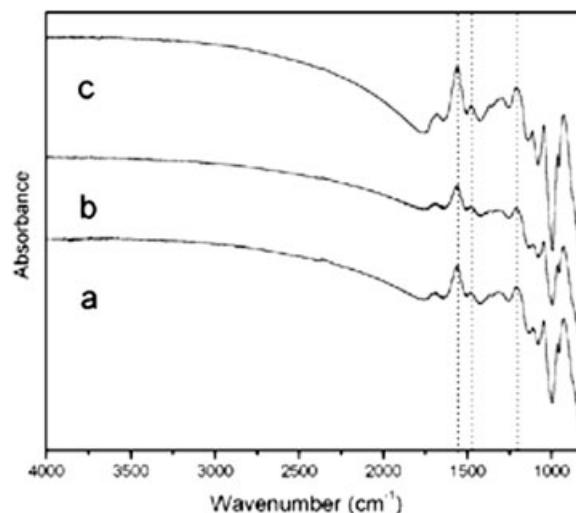


**Figure 12** FTIR spectra of PPy prepared from CTAB/PVP mixed-surfactant solutions with different mass ratios: (a) 2 : 1, (b) 1 : 1, and (c) 1 : 2.

In CTAB/PEG and CTAB/PVP systems, only slight redshifts can be detected, and this can be seen in Figures 11 and 12 and Table I, respectively. This indicates that the nonionic surfactants are not helpful for the improvement of the doping level to a certain degree. On the other hand, the ratios of  $A_2$  to  $A_1$  in CTAB/PVP systems are higher than those in CTAB/PEG systems, and this shows that chain propagation is preferred in CTAB/PVP mixed-surfactant solutions.

PPy prepared from SDS/PEG and SDS/PVP solutions gives high values of  $A_2/A_1$ , especially in SDS/PVP systems (see Figs. 13 and 14 and Table I, respectively). Simultaneously, a redshift from  $1453\text{ cm}^{-1}$  in

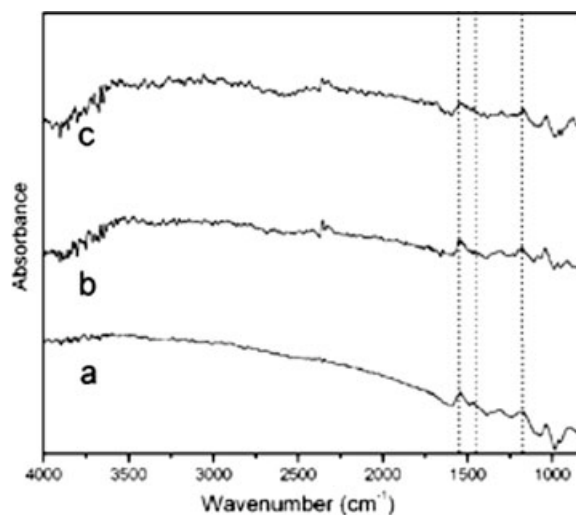


**Figure 13** FTIR spectra of PPy prepared from SDS/PEG mixed-surfactant solutions with different mass ratios: (a) 2 : 1, (b) 1 : 1, and (c) 1 : 2.



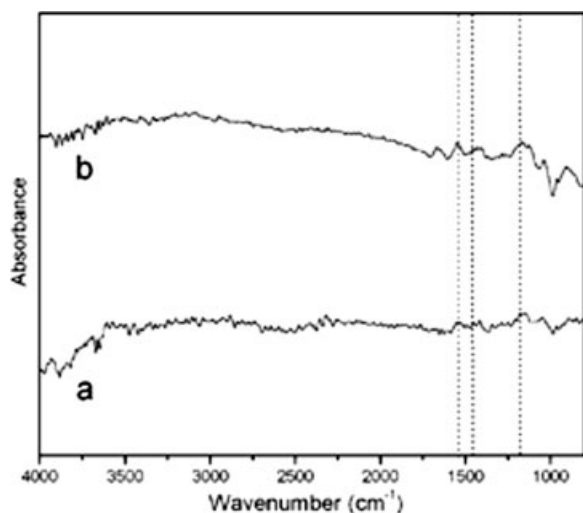


**Figure 14** FTIR spectra of PPy prepared from SDS/PVP mixed-surfactant solutions with different mass ratios: (a) 2 : 1 and (b) 1 : 1.

an SDS solution to  $1431\text{ cm}^{-1}$  in SDS/PVP with a mass ratio of 1 : 1 can be found. We think that the addition of nonionic surfactants reduces the interaction between the anionic surfactant molecules and improves the doping level and chain propagation.

### Conductivity

Figure 15 shows the logarithm of the conductivity versus the ratio of  $A_2$  to  $A_1$  for PPy obtained under different conditions. Baughman and Shacklette developed a simple theoretical model to describe the dependence of the conductivity on the conjugation length for conducting polymers,<sup>19,20</sup> and theoretical lines according to the Baughman–Shacklette theory

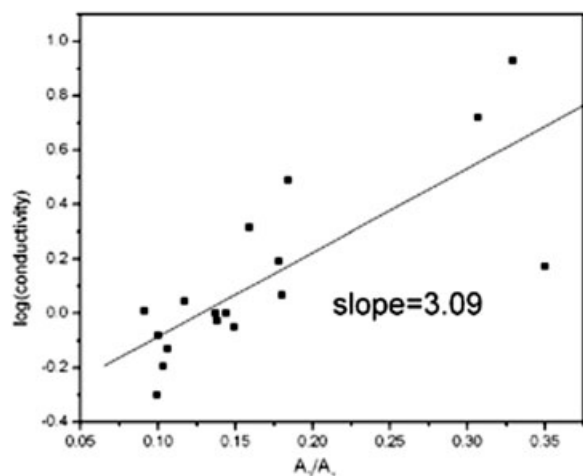


**Figure 15** Plot of the logarithm of the conductivity versus the ratio of the integrated FTIR absorption intensities of the  $1570\text{-}$  and  $1480\text{-cm}^{-1}$  bands ( $A_2/A_1$ ) for PPy prepared under different conditions.

are presented for the regimes of the short conjugation length [slope = 3 in a plot of the logarithm of the conductivity vs  $A_2/A_1$ ] and the long conjugation length ( $2 < \text{slope} < 3$ ). Therefore, according to the simple theoretical treatment introduced in the literature, PPy prepared in these systems is in the regime of the short conjugation length because the slope in Figure 15 equals 3.09, and this is one reason that the resulting PPy preparation in these systems shows relatively low conductivity.

Meanwhile, as can be expected, a high doping level and a high value of  $A_2/A_1$  both result in high conductivity. In Table I, we can find that the conductivity increases with the addition of anionic surfactants, such as SDS and SDSA, although it decreases a bit when a relatively small amount of SDS or SDSA is used. Sample 7 in Table I gives the lowest conductivity of  $0.5\text{ S/cm}$ , which is quite consistent with the datum in the FTIR spectrum. The conductivity of PPy prepared from CTAB/PEG or CTAB/PVP mixed-surfactant solutions does not show much change because of the relatively weak interaction between these surfactants and PPy polycations. When SDS and SDSA are used in a certain large amount, the resulting PPy becomes difficult to be pressed into pellets, and this inhibits the following measurement of the conductivity. However, on the basis of the data in the FTIR spectra, one can deduce that PPy in these systems shows high conductivity.

### CONCLUSIONS

The polymerization of pyrrole was carried out in aqueous solutions in the presence of different types of mixed surfactants. The mixed-surfactant systems included CTAB/SDS and CTAB/SDSA (cationic/anionic), CTAB/PEG and CTAB/PVP (cationic/nonionic), and SDS/PEG and SDS/PVP (anionic/nonionic) solutions, which were superior to the mono-surfactant systems in modulating the morphology and properties of the resulting polymer. PPy showed nanofibers of different lengths when SDS or SDSA was used with CTAB in various molar ratios. Differently sized globular particles were adsorbed onto the nanofibers when PEG or PVP was added to CTAB solutions. Agglomeration was found in the systems with high ratios of SDS or SDSA; however, the nonionic surfactants could weaken the agglomeration to a certain degree. On the other hand, the doping level increased with the usage of anionic surfactants because SDS or SDSA could be incorporated into the structure of the polymer. The resulting PPy with a relatively high doping level and long conjugation chain showed high conductivity, and the PPy prepared in these systems was in the regime of the

short conjugation length according to the Baughman–Shacklette theory.

## References

1. Smela, E.; Gadegaard, N. *Adv Mater* 1999, 11, 953.
2. MacDiarmid, A. G. *Angew Chem Int Ed* 2001, 40, 2581.
3. Saxena, V.; Malhotra, B. D. *Curr Appl Phys* 2003, 3, 293.
4. Otero, T. F.; Boyano, L.; Gortés, M. T.; Vázquez, G. *Electrochim Acta* 2004, 49, 3719.
5. Berdichevsky, Y.; Lo, Y.-H. *Adv Mater* 2006, 18, 122.
6. Huang, J.; Virji, S.; Weiller, B. H.; Kaner, R. B. *Chem—Eur J* 2004, 10, 1314.
7. Lee, Y. H.; Lee, J. Y.; Lee, D. S. *Synth Met* 2000, 114, 347.
8. Jang, K. S.; Lee, H.; Moon, B. *Synth Met* 2004, 143, 289.
9. Zhang, X.; Zhang, J.; Wang, R.; Zhu, T.; Liu, Z. *Chem Phys Chem* 2004, 5, 998.
10. Wu, A.; Kolla, H.; Manohar, S. K. *Macromolecules* 2005, 38, 7873.
11. Zhang, X.; Zhang, J.; Song, W.; Liu, Z. *J Phys Chem B* 2006, 110, 1158.
12. Carswell, A. D. W.; O'Rear, E. A.; Grady, B. P. *J Am Chem Soc* 2003, 125, 14793.
13. Omastová, M.; Trchová, M.; Kovářová, J.; Stejskal, J. *Synth Met* 2003, 138, 447.
14. Zhao, N.; Qi, L. *Adv Mater* 2006, 18, 359.
15. Saunders, B. R.; Saunders, J. M.; Mrkic, J.; Dunlop, E. H. *Phys Chem Chem Phys* 1999, 1, 1563.
16. Bhat, N. V.; Gadre, A. P.; Bambole, V. A. *J Appl Polym Sci* 2001, 80, 2511.
17. Rinaldi, A. W.; Kunita, M. H.; Santos, M. J. L.; Radovanovic, E.; Rubira, A. F.; Girotto, E. M. *Eur Polym J* 2005, 41, 2711.
18. Lu, G.; Li, C.; Shi, G. *Polymer* 2006, 47, 1778.
19. Carrasco, P. M.; Grande, H. J.; Cortazar, M.; Alberdi, J. M.; Areizaga, J.; Pomposo, J. A. *Synth Met* 2006, 156, 420.
20. Baughman, R. H.; Shacklette, L. W. *Phys Rev B* 1989, 39, 5872.